Chemical Geology 460 (2017) 106–116

Contents lists available at ScienceDirect

Chemical Geology

journal homepage: www.elsevier.com/locate/chemgeo

U-Pb geochronology of grossular-andradite garnet

S. Seman[a,*], D.F. Stockli[a], N.M. McLean[b]

[a] Department of Geological Sciences, Jackson School of Geosciences, University of Texas at Austin, TX, USA
[b] Department of Geology, University of Kansas, KS, USA

ARTICLE INFO

Keywords:
Garnet
Grossular-andradite
U-Pb geochronology
LA-ICPMS
ID-TIMS
Skarn
Magmatic-hydrothermal systems

ABSTRACT

This study presents a new laser ablation-inductively coupled plasma mass spectrometry (LA-ICPMS) based U-Pb geochronometric method for dating grossular-andradite (grandite) garnet. Grandite is a primary skarn mineral, therefore dating its growth directly dates hydrothermal activity. As zircon U-Pb geochronometry provides a high-resolution record of magmatic processes, grandite U-Pb dating has the potential to provide a complementary record for hydrothermal systems. This study characterizes four garnets of variable grossular-andradite content and age as potential reference materials for LA-ICPMS U-Pb geochronology: Willsboro Andradite (~1020 Ma, Adirondacks, USA), Red and Yellow Mali Grandite (~200 Ma, Southern Mali) and Lake Jaco Grossular (~35 Ma, Coahuila, Mexico). Isotope dilution-thermal ionization mass spectrometry (ID-TIMS) U-Pb analyses of Willsboro andradite yield a mean $^{206}Pb/^{238}U$ date of 1022 ± 16 Ma. We use Willsboro Andradite as a primary reference material for LA-ICPMS U-Pb characterization of the two other garnets. The non-radiogenic Pb (Pbc) concentration in grandite is variable between specimens. Willsboro Andradite and Mali Grandites contain almost purely radiogenic Pb (Pb*), however Lake Jaco Grossular has a higher Pbc concentration comparatively and yields discordant U/Pb ratios. For specimens with highly variable Pb*/Pbc, linear regression is employed to derive a lower-intercept age. LA-ICPMS U-Pb dates for Yellow Mali Grandite (202 ± 2 Ma; $^{206}Pb/^{238}U$ weighted mean) and Lake Jaco Grossular (35 ± 2 Ma; lower intercept) agree with independent ID-TIMS U-Pb (202.0 ± 1.2 Ma) and (U-Th)/He dates (35 ± 5 Ma) derived for each specimen. The precision of LA-ICPMS U-Pb dates varies between 1–10% (2σ) for the analyzed garnets. Considering the short estimated lifespans of pluton-related hydrothermal systems (tens of thousands to a few million years), Neogene skarns present the best opportunity to test for and resolve separate episodes of garnet growth at these precision levels. As a performance test for the method, we present new U-Pb andradite data from a Late Miocene skarn system on Serifos Island, Greece. This garnet yields a lower-intercept age of 9.15 ± 0.36 Ma, in agreement with biotite Rb-Sr and zircon U-Pb dates from the causative pluton.

1. Introduction

Garnet has the unparalleled ability to record both the conditions and the timing of its growth. The major and trace elemental as well as stable isotopic composition of garnet track changing P-T and fluid conditions throughout growth (Jamtveit et al., 1993; Crowe et al., 2001; D'Errico et al., 2012; Zhai et al., 2014). These conditions can at present be directly linked to absolute timing using Sm-Nd or Lu-Hf geochronology (e.g., Duchêne et al. (1997); Caddick et al. (2010)). Recent analytical advances, including micro-sampling and partial dissolution techniques, have enhanced both the spatial and temporal resolution of Sm-Nd geochronology and its ability to recover detailed P-T-t histories (Harvey and Baxter, 2009; Pollington and Baxter, 2011). Compared to the Sm-Nd system, U-Pb geochronology has a number of distinct advantages. It can be performed using in-situ methods, such as LA-ICPMS or SIMS, and it does not require complementary co-genetic phase or whole rock measurements to calculate an age. This work presents a method to apply U-Pb geochronology, using LA-ICPMS analysis, to grossular-andradite series ($Ca_3Al_2Si_3O_{12}$–$Ca_3Fe_2Si_3O_{12}$) garnets.

The grossular-andradite solid solution series commonly occurs in calcsilicate rocks formed in skarn-type contact metamorphic and hydrothermal environments. From an economic standpoint, many important metals, including Fe, Cu, W, Zn, Mo, etc. are sourced from mineralized skarn deposits (Meinert, 1992). Also, recent studies argue that the formation of skarns may act as a major flux of atmospheric CO_2 throughout geologic history (Lee et al., 2013; Lee and Lackey, 2015). The magmatic-hydrothermal systems which form skarn deposits are inherently short-lived, with geochronologic data suggesting lifespans up to a few million years, while numerical models predict timescales of

* Corresponding author at: Department of Geosciences, Pennsylvania State University, PA, USA.
E-mail address: sxs1194@psu.edu (S. Seman).

http://dx.doi.org/10.1016/j.chemgeo.2017.04.020
Received 3 March 2017; Received in revised form 22 April 2017; Accepted 24 April 2017
Available online 26 April 2017
0009-2541/ © 2017 Elsevier B.V. All rights reserved.

only tens of thousands of years (Maksaev et al., 2004; Deckart et al., 2005; Chiaradia et al., 2013; Chelle-Michou et al., 2015). Metasomatic processes, such as skarn formation, can be indirectly dated by zircon U-Pb geochronology of the causative pluton or cross-cutting dikes (Meinert, 1992; Chiaradia et al., 2013; Yao et al., 2014). Direct dating of magmatic-hydrothermal processes is limited to accessory minerals, including Re-Os of molybdenite, U-Pb of titanite, or Rb-Sr and $^{40}Ar/^{39}Ar$ of micas (Maksaev et al., 2004; Deckart et al., 2005; Chiaradia et al., 2013; Chelle-Michou et al., 2015). These phases are not ubiquitous and the timing of their formation in the overall history of hydrothermal activity is often unclear. Grossular-andradite, however, is a primary product of metasomatism and contains a record of fluid processes in its major, trace, and stable isotope zonation (Jamtveit et al., 1993; Crowe et al., 2001; D'Errico et al., 2012; Zhai et al., 2014). The ability to directly date skarn grandite has the potential to decipher how hydrothermal systems develop through time.

The garnet mineral system has presented a challenge for U-Pb geochronology, in part because almandine, pyrope, and spessartine-rich garnets typically contain less than ~100 ppb U or Th (Haack and Gramse, 1972; Guo et al., 2016). Pioneering garnet U-Pb geochronology on almandine and pyrope-rich garnets from regional metamorphic environments using ID-TIMS proved consistent with other geo/thermochronometers (Mezger et al., 1989 and Mezger et al., 1991), but measurable U and Th within Fe-Mg garnets is likely sourced from inclusions (DeWolf et al., 1996). Grandite-series garnets, on the other hand, contain ppm levels of U and Th (Haack and Gramse, 1972; Lal et al., 1976; DeWolf et al., 1996; Yudintsev et al., 2002). DeWolf et al. (1996) and Meinert et al. (2001) first demonstrated the potential of U-Pb geochronology of grossular-andradite garnet using ID-TIMS methods.

This study uses high-accuracy ID-TIMS U-Pb geochronology to demonstrate U-Pb age homogeneity and reproducibility at the ca. 1% level and to establish a viable primary reference material. We then develop grandite LA-ICPMS U-Pb analytical protocols and demonstrate their efficacy on two other potential reference materials of varying age and composition. The successful methodology is applied to a case study of a Late Miocene skarn system on Serifos Island, Greece associated with a complex intrusive history.

2. Analytical techniques

2.1. ID-TIMS U-Pb geochronology

ID-TIMS U-Pb analyses were conducted at the University of Kansas Isotope Geochemistry Laboratory. Gem-quality, 300–3000 μg garnet fragments of were screened for inclusions under an optical microscope, then placed in ~1 mL of 60 °C ~ 3 N HNO_3 for 12 h to remove any surficial common Pb. Fractions were then spiked with EARTHTIME ^{205}Pb-^{233}U-^{235}U tracer (Bowring et al., 2005; Condon et al., 2015; McLean et al., 2015) and dissolved in ~2 mL of 4:1 mixture of 29 N HF and 7 N HNO_3 on a hotplate set to 180 °C for 48 h. This method was favored over pressure vessel digestion (PDV) due to large fraction size (Krogh, 1973). Pb was isolated from Ca, Al and Fe using an HBr-based ion chromatography in 50 μL Teflon micro-columns loaded with AG1X8 resin (Schmitz and Bowring, 2001). Pb fractions were analyzed on a VG Sector TIMS, employing the Daly detector in peak-hopping mode. Due to insufficient U separation from major elements using AG1X resin, causing poor U ionization on the TIMS, U isotope ratios were measured by solution ID-ICP-MS (Element II at UTChron Labs, University of Texas of Texas at Austin. U and Pb data reduction and uncertainty propagation were performed using Tripoli and ET_Redux software (Bowring et al., 2011; McLean et al., 2011, 2015). Pb isotopic measurements were corrected for lab-derived Pbc by concurrent measurement of procedural blanks. These measurements showed that the total procedural blanks contained the same total Pbc mass as in analyzed garnets, indicating that all common Pb (Pbc) was derived from laboratory blank.

2.2. LA-ICPMS U-Pb geochronology

Internal fragments of garnet specimens ranging in diameter from 1 mm to 5 cm, were embedded in 1-in. epoxy mounts and polished using standard techniques. U-Pb isotope measurements were made using a ThermoFisher Element II, single collector, magnetic sector ICP-MS together with a Photonmachines Analyte G2 193 nm ArF excimer laser at UTChron, University of Texas at Austin. The Analyte G2 excimer is fitted with a large format, two-volume Helex cell. Laser working conditions were similar to those used for zircon analyses at UTChron: 30 s ablation time, 10 Hz repetition rate, 6 mJ energy, 17% beam attenuation, resulting in a fluence of 1.67 J cm^{-2}. He carrier gas and Ar sample gas flow rates were both set at ~1 L/min. ^{202}Hg, ^{204}Pb, ^{206}Pb, ^{207}Pb, ^{208}Pb, ^{232}Th, ^{235}U, and ^{238}U were analyzed by cycling of the electrostatic analyzer, EScan mode, at a static magnet mass. Unlike typical accessory mineral analyses, a 110 μm spot size was employed to maximize count rates and optimize precision. High relative spatial resolution is maintained, however, as analyzed garnets were typically several millimeters or larger in diameter. The mass spectrometer method used is identical to the zircon and rutile U-Pb method employed at UTChron (Smye and Stockli, 2014; Hart et al., 2016; Marsh and Stockli, 2015), with one change: ^{238}U is measured in counting mode on the SEM detector as opposed to analog mode due to < 5 ppm U abundances. This makes calibration of the detector, deadtime and linearity, more influential, so these were determined in solution mode using natural $^{238}U/^{235}U = 137.88$.

Garnet U-Pb ICP-MS data was reduced using the VizualAge data reduction scheme (Petrus and Kamber, 2012) for Iolite software (Paton et al., 2011). Willsboro Andradite, used as a primary U-Pb standard, showed consistent elemental fractionation behavior, allowing for a standard downhole fractionation correction. Based on the percentage of Pbc present, final sample dates were calculated one of two ways: 1) Samples which yield concordant data ($(1 - (^{206}Pb/^{238}U \text{ date}) / (^{207}Pb/^{206}Pb \text{ date}) < 0.1$), are reported as $^{206}Pb/^{238}U$ weighted mean dates. 2) Samples with significant Pbc are reported as lower intercept dates.

2.3. (U-Th)/He thermochronology

(U-Th)/He thermochronometric dates of garnet were also used to corroborate LA-ICPMS U-Pb dates. Individual fractions, consisting of multiple garnet fragments, were loaded into 3 mm × 2 mm platinum tubes. Total fraction sizes ranged between 500 μg–1500 μg. After loading into the He extraction line (UTChron Labs, University of Texas at Austin), samples are heated to approximately 1300 °C for 10 min using a diode laser following procedures outlined in Tagami et al. (2003). Multiple heating cycles are typically necessary in order for extractions to reach < 1% of the total He, similar to other retentive phases (e.g. zircon, magnetite) (Reiners, 2005; Blackburn et al., 2007). Extracted ^{4}He is mixed with a ^{3}He spike and cryogenically purified before being measured by a quadrupole noble gas mass spectrometer. Moles ^{4}He in garnets were calculated by isotope dilution using a manometrically calibrated ^{4}He standard.

Following laser heating, fractions were removed from platinum packets and spiked with a 7 N $HN0_3$ based ^{235}U-^{230}Th-^{149}Sm tracer. Fractions were dissolved in a 5:1 HF-HNO_3 mixture heated to approximately 180 °C for 12 h then and brought back into solution using 12 N HCl, and heated again at 180 °C for 12 h. U, Th, and Sm were measured using solution ID-ICP-MS (Element II at UTChron Labs, University of Texas of Texas at Austin).

2.4. Major and trace element analysis

Major element garnet compositions were determined by electron microprobe analysis (EPMA) using the JEOL JXA-8200 at the Department of Geological Sciences, University of Texas at Austin.

Garnet compositions reported are the average of spot analyses taken on garnet fragments (Lake Jaco, Mali Grandite, Serifos Andradite) or transects across whole garnets (Willsboro Andradite). Trace element and REE concentrations were measured by LA-ICPMS at UTChron Labs, Department of Geological Sciences, University of Texas at Austin. Laser working conditions were identical to U-Pb determinations except for a smaller, 40 μm laser spot size. ^{29}Si was used as an internal standard, based on mean Si concentrations of garnets from EPMA analysis, and NIST612 standard glass as a primary standard (Norman et al., 1996) to determine elemental fractionation and instrument drift. Raw data were reduced using the Trace Element_IS data reduction scheme of Iolite software (Paton et al., 2011).

3. Grossular-andradite garnet: potential reference material

3.1. Willsboro Andradite, NY, USA

This specimen is sourced from the Willsboro wollastonite deposit within the Adirondack Highlands Province. This skarn formed proximal to the Marcy Massif Anorthosite, emplaced at 1155 ± 5 Ma (Clechenko et al., 2002; Hamilton et al., 2004). The Marcy Massif is part of the greater Anorthosite-Mangerite-Charnockite-Granite Suite which intruded Grenville-age metamorphic provinces from 1180 to 1130 Ma (McLelland et al., 1996). The anorthosite and its associated skarns were later metamorphosed at granulite facies conditions during the Ottawan Orogeny between ~1090–1035 Ma (Valley et al., 1990; McLelland et al., 2001). A meteoric $\delta^{18}O$ signature in garnet led Valley (1985) and Clechenko and Valley (2003) to conclude that the Willsboro and Lewis skarns were formed at < 10 km depth in the crust, before recrystallization and homogenization under granulite facies conditions. The Willsboro garnet analyzed for this study are ~0.5 cm diameter, near end-member andradite, Grs10 And90, intergrown with coarse wollastonite that do not preserve oscillatory growth zonation (Fig. 1). Rarely cm-diameter garnets retain their original oscillatory zonation

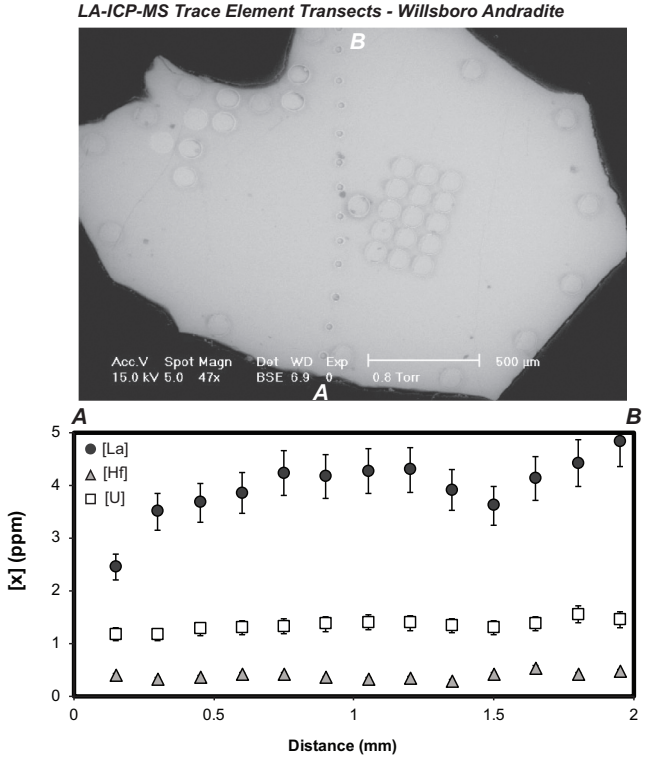

Fig. 1. BSE images of Willsboro andradite. Few inclusions are observed in these garnets and they show consistent major element composition. Laser ablation pits, (110 μm and 40 μm) are shown in the first image.

(Clechenko and Valley, 2003). Sm-Nd multi-mineral geochronology (calcite + wollastonite + diopside + garnet) from a similar skarn in the nearby Lewis wollastonite deposit record Ottawan dates (1035 ± 40 Ma) (Basu et al., 1988).

3.2. Mali grandite, Mali

The garnet specimens we call Mali grandite. is sourced from alluvial deposits in southern Mali discovered in 1994, but little is reported about its geologic origin (Johnson et al., 1995) One likely source is skarn produced by dikes which intrude carbonates throughout much of the region (Furon et al., 1963; Verati et al., 2005). These intrusions range from Permian to Jurassic in age, but are predominantly related to Central Atlantic Magmatic Province (CAMP) activity at the Triassic-Jurassic boundary (Furon et al., 1963; Verati et al., 2005). Large volumes of ~200 Ma flood basalts are exposed throughout nearby Guinea and Senegal (Marzoli et al., 1999) and are likely correlative to those present in Mali. Also, dike swarms of identical age are exposed in northern Mali (Sebai et al., 1991).

Two Mali grandite specimens, yellow and red, were analyzed in this study. Mali yellow garnets are bright yellow, ~1 cm diameter anhedral fragments with a composition of Grs75 And25 (Table 1). Mali Red is a ~3 cm diameter, dark red, euhedral garnet crystal with an average composition of Grs37 And52. Oscillatory zonation is not apparent in analyzed samples optically or using back-scattered electron (BSE) imaging. While fluid inclusions are present throughout the specimens, mineral inclusions are not observed.

3.3. Lake Jaco grossular, Coahuila, Mexico

Lake Jaco grossular is the market name for grossular-rich garnets sourced from the Sierra de Cruces Range, east of Laguna de Jaco, on the border of the Mexican states of Chihuahua and Coahuila (Rocha et al., 1986). Skarn, consisting of garnet + vesuvianite + quartz + wollastonite, is developed in Cretaceous limestone intruded by a diorite body of indeterminate age (Rocha et al., 1986). No published age data exists for the causative diorite intrusion, but, regional plutons range from Eocene to Oligocene in age (Bloomfield and Cépeda-Dávila, 1973). In the nearby Big Bend region of Texas, igneous activity spans from ~48–17 Ma, with the most extensive magmatism occurring between 38 and 32 Ma (Barker, 1977; Henry and Price, 1984).

Lake Jaco is widely available and, as an end-member grossular, commonly employed in mineralogical studies. It varies compositionally between andradite and grossular end members and andradite-rich cores of variable size are common. A ~3 cm diameter cream-colored garnet of average composition Grs85 And15 was chosen for analysis.

4. Case study

4.1. Serifos Island, Cyclades, Greece

Contact metamorphism and skarn formation are inherently short-lived processes on geologic time scales (Maksaev et al., 2004; Chiaradia et al., 2013; Chelle-Michou et al., 2015). As the relative precision of our garnet U-Pb technique ranges from 1 to 10% (2σ), younger dates have smaller absolute uncertainties. Neogene skarns therefore represent the best opportunity to resolve episodic mineral growth in the short lifespans of magmatic-hydrothermal systems. On Serifos Island, Greece, a Late Miocene granodiorite intrudes the Cycladic Blueschist Unit (CBU), forming extensive skarn (Marinos, 1951; Salemink, 1985; Salemink and Schuiling, 1987; Ducoux et al., 2017). The CBU is a collection of poly-metamorphosed volcanics, carbonates and siliciclastic sedimentary rocks that experienced blueschist facies metamorphism in the Eocene followed by greenschist facies retrogression in the middle Miocene (Dürr et al., 1978; Altherr et al., 1982). Magnetite ore is present within calcic iron skarn formed primarily within marbles of

Table 1
Sample localities for grossular-andradite garnet employed in this study. Includes LA-ICPMS based estimates of [U] and [Th] contents.

Sample name	Locality	Grs	And	U (ppm)	2S.D.	Th (ppm)	2S.D.
Lake Jaco Grossular	Sierra de Cruces Range, Coahuila, Mexico	84	16	1.7	0.3	3.2	0.4
Mali Grandite Yellow	Southern Mali, Africa	72	28	2.0	0.5	2.0	1.6
Mali Grandite Red	Southern Mali, Africa	37	52	7.0	6.8	3.3	6.8
Serifos Andradite	Serifos Island, Cyclades, Greece	0	100	9.3	13.6	0.1	0.2
Willsboro Andradite	Adirondacks, New York, U.S.A.	10	90	1.0	0.5	0.8	0.5

western Serifos (Marinos, 1951; Salemink, 1985). Hedenbergite-andradite-magnetite skarn also formed proximal to the pluton hosted within mafic orthogneisses of the CBU (Salemink, 1985). End-member composition andradite forms cm-scale veins both parallel to and cross-cutting the foliation. Garnet analyzed in this study was sampled from foliation-parallel veins within a mafic orthogneiss (N37.17414° E024.49221°). ID-TIMS U-Pb zircon data from the pluton as well as both deformed and nondeformed dacitic dykes range in age from 11.6 to 9.5 Ma (Iglseder et al., 2009). Rb-Sr biotite dates, ranging from 7.7–8.5 Ma, provide a lower boundary for cooling of the pluton below ~400 °C (Iglseder et al., 2009). Direct dating of andradite garnet has the potential to provide tighter age constraints on skarn formation over this 2 m.y. timespan. Furthermore, the Serifos locality acts as an ideal performance test for grandite U-Pb geochronology in Miocene and younger cases.

5. Results

5.1. ID-TIMS

ID-TIMS analysis of *Willsboro Andradite* produces < 1% discordant U-Pb ratios after ^{204}Pb correction. Based on analyses of procedural blanks containing similar amounts of Pbc, measured Pbc not sourced from analyzed garnet. The Willsboro Andradite U-Pb data show more scatter than can be explained by analytical uncertainties alone. For instance, the weighted mean of Willsboro ^{206}Pb/^{238}U age has an MSWD of 46. Instead of assuming that this data comprises repeat measurements of a single true value, a mean and overdispersion models the true data as being normally distributed around a mean value, with the overdispersion parameter estimating this scatter (Vermeesch, 2010). This 'excess scatter' should be included in the uncertainty in primary standard calibration (Horstwood et al., 2016). We calculate the mean and overdispersion of the ^{206}Pb/^{238}U dates of the Willsboro Andradite to be 1022 ± 16 Ma (2σ overdispersion; n = 9) (Fig. 2B). Forty-five individual fractions were dissolved and U and Pb purification attempted using column chemistry techniques. Thirty-two of the analyzed Pb fractions were rejected based on a lack of detectable counts for all Pb isotopes or due to high Pbc content (^{206}Pb/^{204}Pb < 50). The remaining four fractions were excluded due to negative or positive discordancy (> 2%).

ID-TIMS analysis of *Mali Red/Yellow Grandite* yielded 4 analyses with < 1% discordant U-Pb ratios after ^{204}Pb correction of Pbc. Similar to Willsboro Andradite, procedural blanks contained similar amounts of Pbc to garnet, suggesting all measured Pbc is lab-derived. The weighted mean of ^{206}Pb/^{238}U dates is 202.0 ± 1.2 Ma (MSWD = 1.6; n = 4) (Fig. 2B) (Table 2). Due to the low MSWD of this date, we report weighted mean rather than overdispersion as with Willsboro Andradite. Similar to Willsboro Andradite, 19 of the twenty analyses of Mali Yellow were rejected as no Pb was detected on the Daly Counter or measured ^{206}Pb/^{204}Pb were < 50. Four of seven fractions of Mali Red were rejected based on the same grounds. The reported date represents a composite of three Mali Red analyses and one Mali Yellow analysis.

5.2. LA-ICPMS

All reported LA-ICPMS age data acquired used Willsboro Andradite as a primary age reference standard. The ID-TIMS data employed are ^{204}Pb corrected. ^{206}Pb/^{238}U downhole fractionation correction from this LA-ICPMS analytical session is shown in Fig. 3. ^{206}Pb/^{238}U ratios show reproducibility similar to zircon U-Pb standards and do not require more complex fractionation correction schemes.

Mali Yellow yields age data in excellent agreement with ID-TIMS data derived for Mali Red and Mali Yellow (Fig. 3B, Fig. 5). The calculated final age by a weighted mean of ^{206}Pb/^{238}U date is 202.0 ± 2.0 Ma (MSWD = 1.5, n = 25) (Fig. 5). U and Th concentrations are at 2.0 ± 0.5 ppm (2S.D.) and 2.0 ± 1.6 ppm (2S.D.) (Table 1) (Fig. 6). At the mm-scale [U] and [Th] are not correlated with [Ce] or [Hf] (Fig. 6). *Mali Red Grandite* did not yield reproducible ^{207}Pb/^{235}U ratios when using Willsboro Andradite as a primary

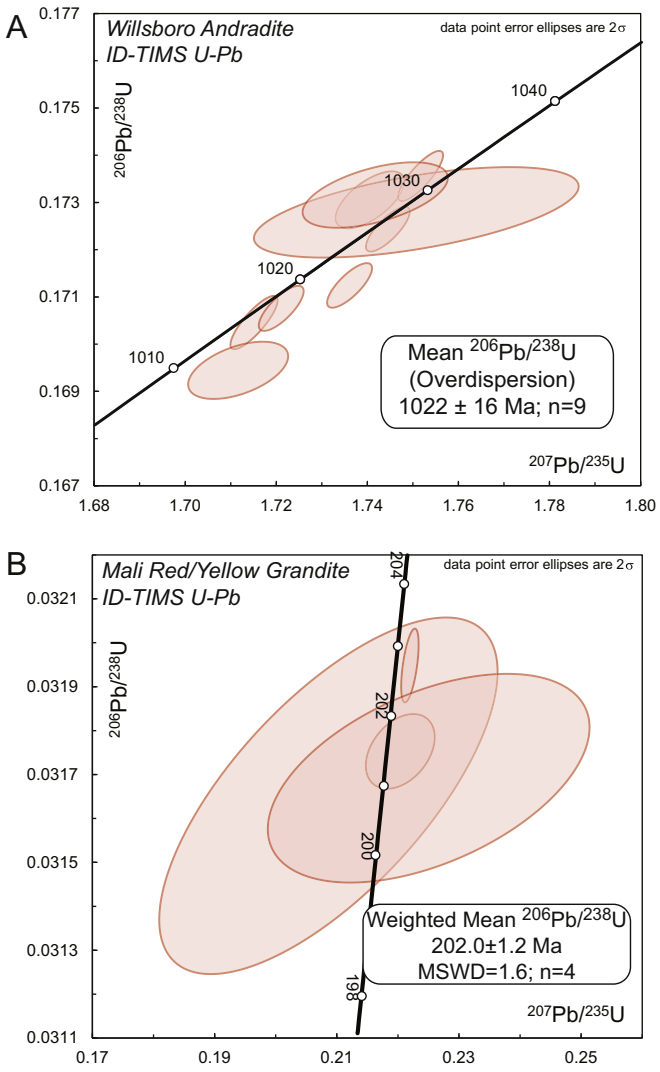

Fig. 2. A) ID-TIMS age results for Willsboro andradite. B) ID-TIMS age results for Mali grandite. Isotopic measurements are corrected for lab-derived Pbc by concurrent measurement of procedural blanks. No correction of initial Pbc in garnet is included.

Table 2
ID-TIMS results for Willsboro Andradite and Mali Grandite. All ratios and dates are corrected for lab blank Pbc. Data do not include correction for initial Pbc in garnet.

Grossular Andradite ID-TIMS U-Pb data

Willsboro Andradite Fraction	U (ppm)	Pb (ppm)	$^{207}Pb/^{235}U$	± 2S.E.	$^{206}Pb/^{238}U$	± 2S.E.	Pb* (pg)	Pbc (pg)	Pb*/Pbc	$^{206}Pb/^{204}Pb$	± 2S.E.	Th/U	$^{206}Pb/^{238}U$ age	± 2S.E.	$^{207}Pb/^{235}U$ age	± 2S.E.	$^{206}Pb/^{207}Pb$ age	± 2S.E.	RHO
G9	1.85	0.38	1.7361	0.0040	0.17124	0.00038	430	21	20.5	1158.6	2.8	0.83	1018.9	2.3	1022.0	2.4	1028.5	5.0	0.77
G10	1.51	0.30	1.7151	0.0042	0.17046	0.00046	535	22	24.0	1362.8	4.0	0.80	1014.5	2.7	1014.1	2.6	1013.2	4.7	0.82
G12	1.54	0.32	1.7211	0.0040	0.17076	0.00039	545	29	18.6	1041.3	2.6	0.82	1015.8	2.3	1016.0	2.6	1016.4	5.5	0.74
G15	1.29	0.27	1.7406	0.0062	0.17306	0.00049	1013	61	16.6	912.2	2.8	0.83	1027.8	2.9	1022.7	3.5	1011.7	8.1	0.69
G16	1.61	0.33	1.7445	0.0039	0.17244	0.00039	560	28	20.2	1131.5	2.8	0.82	1025.1	2.3	1024.8	2.5	1024.1	5.1	0.76
G17	1.45	0.30	1.7176	0.0091	0.17391	0.00133	1027	47	21.7	1188.3	9.8	0.83	1032.8	7.9	1014.4	5.4	975	18	0.46
G20	1.28	0.26	1.7517	0.0040	0.17356	0.00043	794	33	24.0	1328.0	3.6	0.83	1031.2	2.6	1027.4	2.5	1019.2	4.5	0.82
G22	1.65	0.36	1.7116	0.0090	0.16945	0.00049	433	57	7.7	434.9	1.4	0.77	1006.7	3.0	1010.8	5.0	1020	13	0.59
G36	1.10	0.35	1.7508	0.0291	0.17279	0.00078	200	120	1.7	110.9	0.5	0.82	1027.5	4.6	1027	17	1027	49	0.57
G39	1.67	0.42	1.7417	0.0130	0.17316	0.00057	507	134	3.8	227.1	0.8	0.83	1029.5	3.4	1024.1	7.7	1013	21	0.53

Mali Grandite Fraction	U (ppm)	Pb (ppm)	$^{207}Pb/^{235}U$	± 2S.E.	$^{206}Pb/^{238}U$	± 2S.E.	Pb* (pg)	Pbc (pg)	Pb*/Pbc	$^{206}Pb/^{204}Pb$	± 2S.E.	Th/U	$^{206}Pb/^{238}U$ age	± 2S.E.	$^{207}Pb/^{235}U$ age	± 2S.E.	$^{206}Pb/^{207}Pb$ age	± 2S.E.	RHO
Yellow																			
G27	7.55	0.65	0.2086	10.8439	0.03165	1.04763	55	81	0.7	57.9	0.6	0.75	200.9	2.1	192	19	90	240	0.70
Red																			
D1	4.40	0.17	0.2204	2.0900	0.03175	0.21867	222	63	3.5	252.3	0.6	0.17	201.5	0.4	202.2	3.8	211	47	0.38
D3	6.99	0.23	0.2220	0.5237	0.03195	0.21480	316	26	12.1	833.4	1.8	0.14	202.7	0.4	203.5	1.0	213	10	0.57
D6	6.77	0.43	0.2250	9.5602	0.03169	0.61232	183	204	0.9	77.6	0.5	0.17	201.1	1.2	206	18	263	210	0.49

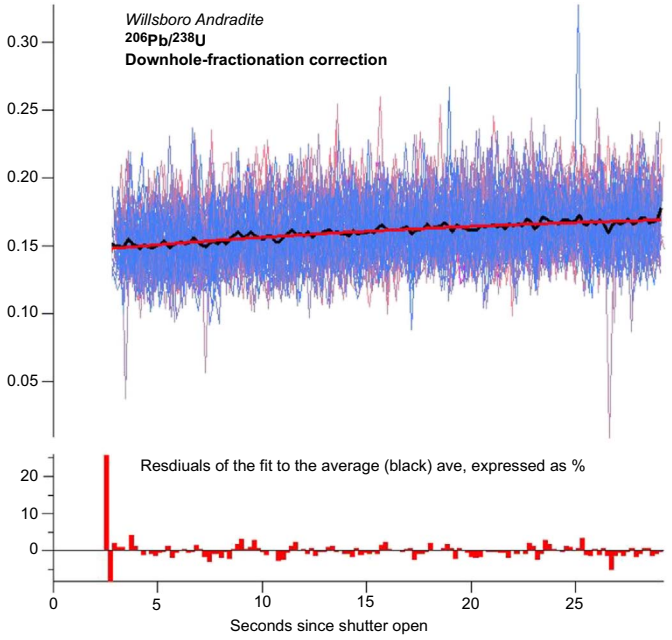

Fig. 3. Downhole fractionation correction (DFC) using Willsboro Andradite. $^{206}Pb/^{238}U$ ratios are reproducible, resulting in a well-behaved correction similar to zircon U-Pb standards.

standard.

LA-ICPMS U/Pb determinations for *Lake Jaco Grossular* were variable and generally discordant due to the presence of Pbc, but form a linear array. Linear regression using Tera-Wasserburg concordia yields a lower intercept date of analyses is 35.0 ± 1.4 Ma (MSWD = 0.93; n = 18) (Fig. 4). (U-Th)/He age data agrees with LA-ICPMS U-Pb data (Fig. 4). The average date of 9 analyses is 35 ± 5 Ma (2S.D.). U and Th concentrations are consistent, similar to Mali Grandite, at 1.7 ± 0.3 ppm (2S.D.) and 3.2 ± 0.4 ppm (2S.D.) (Table 1). At the mm-scale [U] and [Th] are not correlated with [Ce] or [Zr].

Serifos Andradite U-Pb data are highly discordant and span almost the entirety of Tera-Wasserburg space, with many analyses containing predominantly Pbc while others are highly radiogenic. The lower intercept date for all analyses based on linear regression is 10 ± 1 Ma (MSWD = 112; n = 42) (Fig. 8). While Serifos Andradite contains large percentages of Pbc, it also possesses the second highest, but most variable U concentrations of any garnets measured in this study, ranging from 5 to 30 ppm. Th concentrations are lower ranging from 10 to 400 ppb (Table 1) (Fig. 7).

6. Discussion

6.1. Age interpretation: potential reference material

For *Willsboro Andradite*, this work determined a weighted average $^{206}Pb/^{238}U$ date for ID-TIMS analysis of 1022 ± 8 Ma. This agrees with Sm-Nd multi-mineral data of Basu et al. (1988) (1035 ± 40 Ma). Both published Sm-Nd and these new U-Pb ID-TIMS dates are approximately 150 m.y. younger than zircon U-Pb age data for the Marcy Massif Anorthosite (1155 ± 5 Ma) (Clechenko et al., 2002; Hamilton et al., 2004). This discrepancy between U-Pb and Sm-Nd dates and zircon U-Pb dates from the Marcy Massif suggests that Willsboro garnet must have recrystallized or been diffusionally reset under granulite-facies conditions during the Ottawan orogeny. Mezger et al. (1989) originally estimated the diffusivities of U^{4+} and Pb^{2+} in garnet to be slower than the more well-constrained cations of Sm^{3+} and Ca^{2+}, suggesting a closure temperatures for the U-Pb system in excess of 800 °C for ~0.5 cm diameter grains. However, more detailed work on the diffusion kinetics of U and Pb in garnet would be required to differentiate between recrystallization and diffusional loss of Pb in this setting.

Dispersion of U-Pb dates for Willsboro andradite may be the result of Pb-loss or multiple recrystallization events. Younger Willsboro

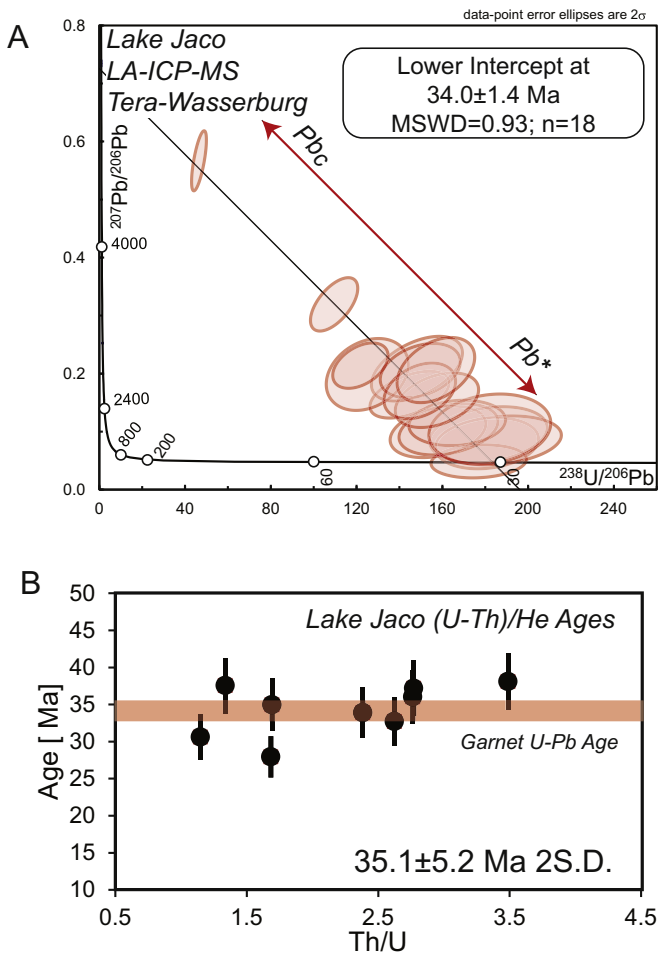

Fig. 4. A) LA-ICPMS U-Pb results from Lake Jaco Grossular plotted in Tera-Wasserburg concordia using Willsboro Andradite as a primary standard. The lower intercept age derived from this regression is 35.0 ± 1.4 Ma. B) (U-Th)/He dates from Lake Jaco Grossular agree with U-Pb dates (Seman et al., 2014).

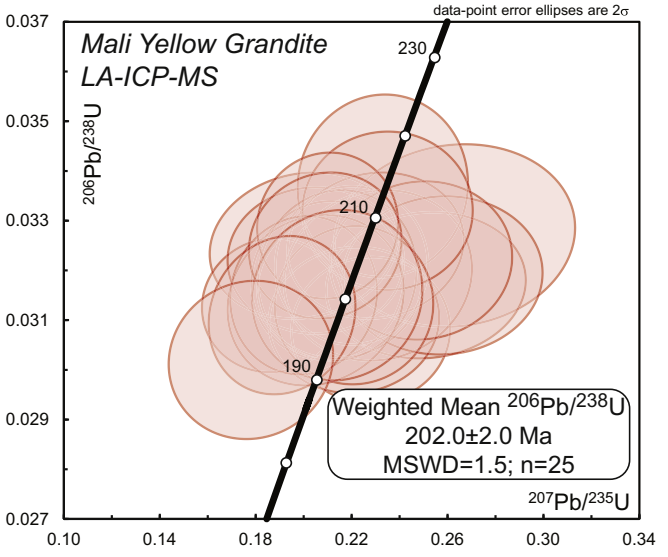

Fig. 5. LA-ICPMS age results for Mali Yellow Grandite using Willsboro Andradite as a primary standard. These ages agree exactly with the Mali Grandite ID-TIMS ages.

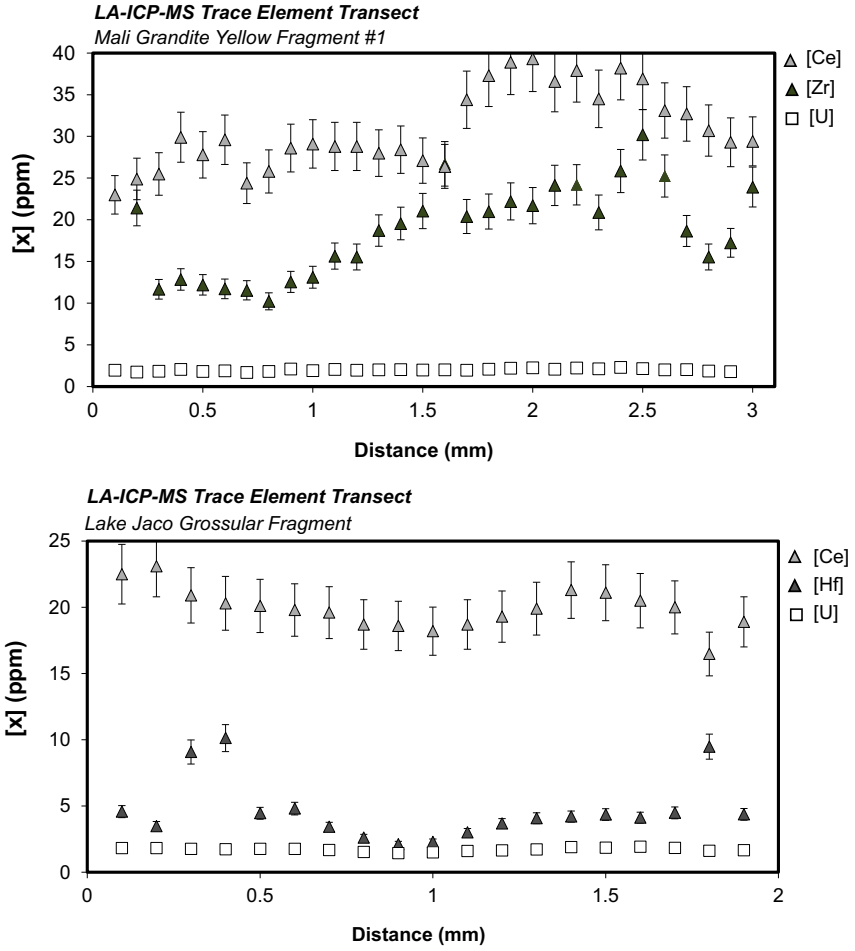

Fig. 6. LA-ICPMS trace element transects of fragments of Mali Yellow Grandite and Lake Jaco Grossular across lateral distances of 2–3 mm. [U] is reproducible and is not correlated with increasing [Zr], [Hf], or [Ce]. Inclusions, such as zircon or monazite, are not contributing to observed [U] at this scale.

analyses appear to scatter linearly off of concordia, suggesting Pb-loss. Multiple recrystallization events under granulite-metamorphism may also be responsible for the dispersion of Willsboro dates. If these younger, more discordant analyses are excluded, this results in an age of 1128 ± 2 Ma. This study does not report this as a reference age for LA-ICP-MS standardization, however. The full range of analyses is preferred in order to best represent the range of isotopic values derived from the sample.

LA-ICPMS and ID-TIMS methods produce U-Pb dates in agreement with one another for *Mali Red/Yellow* (202 ± 2 Ma and 202.0 ± 1.2 Ma, respectively). These age determinations are corroborated by $^{40}Ar/^{39}Ar$ data from CAMP-related basaltic dikes in northern Mali (Verati et al., 2005) as well as extensive flood basalts located to the west in Guinea and Senegal (Sebai et al., 1991; Marzoli et al., 1999). Mali Grandite accurately records the timing of its formation based on its overall agreement geochronology throughout the region. These Triassic-Jurassic garnet U-Pb dates confirm CAMP-related intrusions and their related skarns to be the likely source for these placer garnets.

This study determined ages for *Lake Jaco Grossular* by the use of two separate geochronometric systems, U-Pb and (U-Th)/He, which yield consistent results. A LA-ICPMS U-Pb lower intercept date of 34 ± 1.4 Ma agrees well with (U-Th)/He results which give a date of 35 ± 5 Ma. No geochronologic age data exists for the diorite body of the Las Cruces range. However, these age determinations coincide with extensive volcanism throughout northern Mexico and the proximal Big Bend region of Texas (Clark et al., 1982). Interestingly, (U-Th)/He and U-Pb dates overlap within error. Currently, closure temperature estimates for diffusive loss of He in garnet range from 200 to 300 °C (Blackburn, 2006; Seman et al., 2014). Considering the percent level errors of both U-Pb and (U-Th)/He data, overlap between U-Pb and (U-Th)/He in skarn systems is not unexpected in short-lived skarn systems, especially when they are intruded into the shallow crust (< 10 km depth) and cool quickly (Chiaradia et al., 2013).

6.2. Age interpretation: Serifos Island

Serifos Andradite LA-ICPMS data are highly discordant and span a wide range of Tera-Wasserburg space. The lower intercept age defined by this array is 10 ± 1 Ma (MSWD = 112; n = 43). This date agrees with the U-Pb, (U-Th)/He, and $^{40}Ar/^{39}Ar$ data from the Serifos Granodiorite (Iglseder et al., 2009; Grasemann et al., 2011). Zircon U-Pb dates from pluton and dykes range in age from 9.6–11.5 Ma in age. Iglseder et al. (2009) assigned the source of this dispersion to either zircon inheritance or late fluid flow and Pb loss. Rb-Sr biotite dates from the pluton produces a range of 8.5–7.7 Ma. A CBU mylonite proximal to our garnet U-Pb sample yields a $^{40}Ar/^{39}Ar$ mica age of 8.9 ± 0.1 Ma (Grasemann et al., 2011). Average ages of zircon (U-Th)/He samples across the island range from 5.8–8.0 Ma (Grasemann et al., 2011).

Although this andradite U-Pb data is consistent with existing data sets, its precision limits interpretation as to the timing of skarn formation relative to pluton emplacement. The principal source of uncertainty in this data set originates from analyses with $^{238}U/^{206}Pb < 200$. Dispersion of $^{207}Pb/^{206}Pb$ analyses with $^{238}U/^{206}Pb < 200$ may be due to Pb-rich inclusions not observable in BSE or heterogeneous $^{207}Pb/^{206}Pb$ in the garnet itself. If only

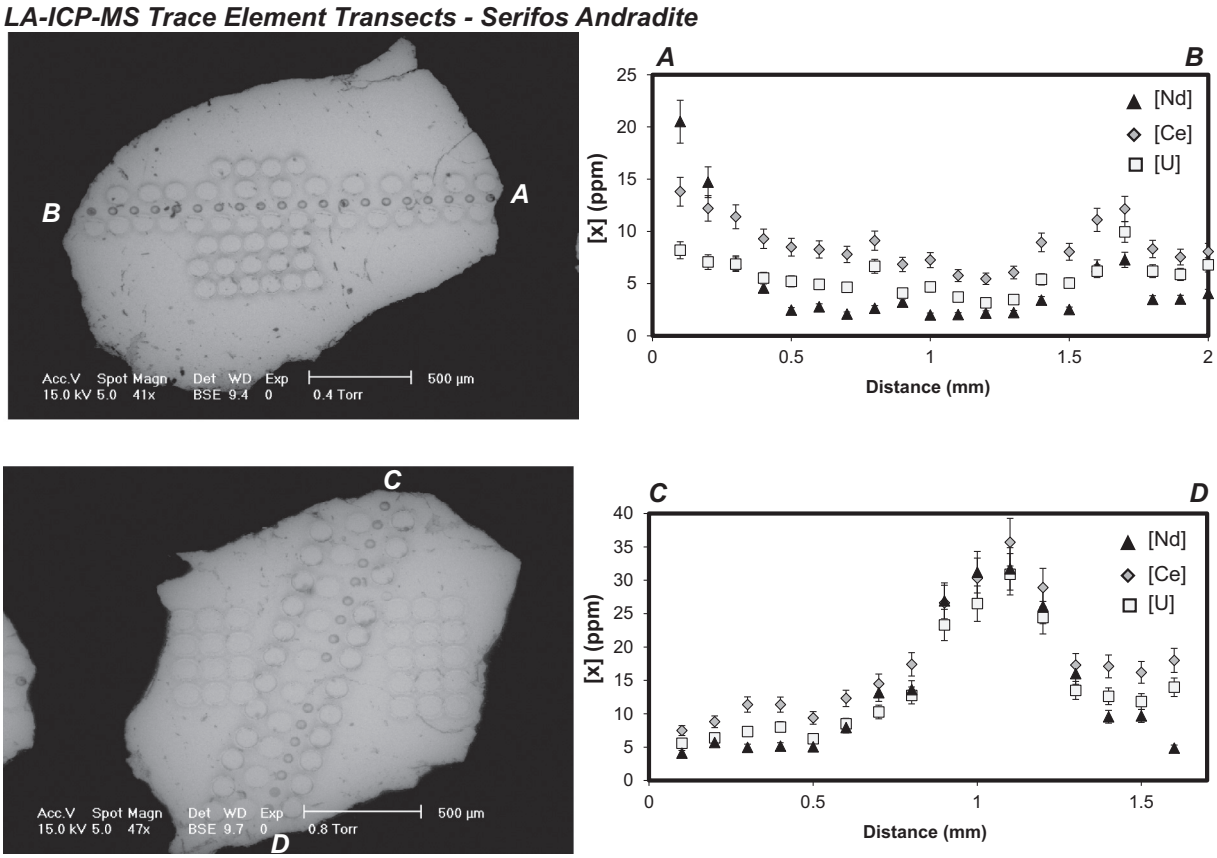

Fig. 7. BSE images of analyzed fragments of Serifos Andradite. 110 µm ablation pits are used for U-Pb age analyses and smaller 40 µm pits for trace element analyses. LA-ICPMS trace element transects of two fragments of Serifos Andradite, correlating to previous BSE images. [U] is variable across fragments, correlating with [Ce] and [Nd]. [Zr] and [Hf] were at instrument detection limits (~500 ppb and ~30 ppb, respectively). No BSE bright inclusions are observed and trace element zonation appears to be at a scale of ~0.5 mm. Inclusions, therefore, are not a significant source of [U] are this scale.

analyses with $^{238}U/^{206}Pb > 200$ are considered they define a well-behaved array with a lower intercept of 9.15 ± 0.36 Ma (MSWD = 0.9; $n = 13$) (Fig. 8). This second, more precise age determination, falls directly in between the youngest zircon U-Pb dates and Rb-Sr age data from the Serifos Granodiorite. LA-ICPMS trace element transects and BSE imagery of the analyzed fragments do not point to inclusions as a major source of [U]. Although [U] is correlated with [Ce] and [Nd], this zonation is at the mm-scale (Fig. 7).

This data suggests that skarn formation occurred, at least partially, in the Late Miocene on Serifos Island, concurrent with the youngest intrusion activity recorded by zircon U-Pb. Most importantly, this demonstrates that the grandite U-Pb method has the precision to yield a resolvable age from magmatic crystallization (zircon U-Pb) and thermochronometric data which record cooling of plutonic rocks and the hydrothermal system. At this point it is difficult to say conclusively whether these U-Pb dates best represent crystallization of garnet or cooling of the hydrothermal system, however. Following estimates of closure temperature from Mezger et al., 1989, this data would best represent crystallization of garnet. However, more detailed work examining major and trace element zonation in grandite and comparing thermochronometry data from the same rock sample is necessary to infer the diffusivities of U and Pb in grossular-andradite garnet.

6.3. Potential LA-ICPMS reference material

The ideal U-Pb reference material possesses reproducible, low variance U-Pb ratios. Analyses of common Pb rich accessory phases, particularly apatite and allanite, are often complicated by the fact that reference material with uniform U-Th-Pb ratios is not easily found (Chew et al., 2014). Pbc concentrations vary considerably throughout these minerals, leading to non-uniform U-Pb ratios and the inability to perform a simple fractionation correction. Fortunately, from the small sampling of grandite studied herein, two samples produce consistently concordant analyses containing low percentages of Pbc, Mali Yellow Grandite and Willsboro Andradite. The relatively high-concentrations of Pb in Willsboro Andradite makes it preferable to the low [U] Mali Yellow. The young age and highly variable U-Pb ratio of Lake Jaco Grossular make it a poor standard, but, as it is widely available, it may prove a useful secondary standard.

For garnets which contain single ppm [U], Willsboro Andradite preformed well as a primary standard, but yields inaccurate $^{207}U/^{235}U$ age data for the higher [U] Mali Red. This discrepancy is likely due to SEM detector calibration (deadtime and analog correction factor), as Mali Red TIMS U-Pb dates agree with Mali Yellow LA-ICPMS U-Pb dates. Based on this, the higher [U] Mali Red may be a preferable standard for garnets containing > 15 ppm [U], but will require more extensive characterization and testing similar to Mali Yellow.

For future grossular-andradite U-Pb geochronology, more numerous and precise ID-TIMS U-Pb age are necessary to term them 'well-characterized standards'. Currently, the major source of uncertainty and inconsistency in ID-TIMS data is likely the dissolution and column chemistry method. Although ID-TIMS and LA-ICPMS data presented herein are self-consistent, more precise reference ages are required to improve the accuracy of the fractionation correction and unknown age determinations.

6.4. Applications

To determine the age of skarn formation where no other age constraints are present, U-Pb zircon age data taken from the genetically

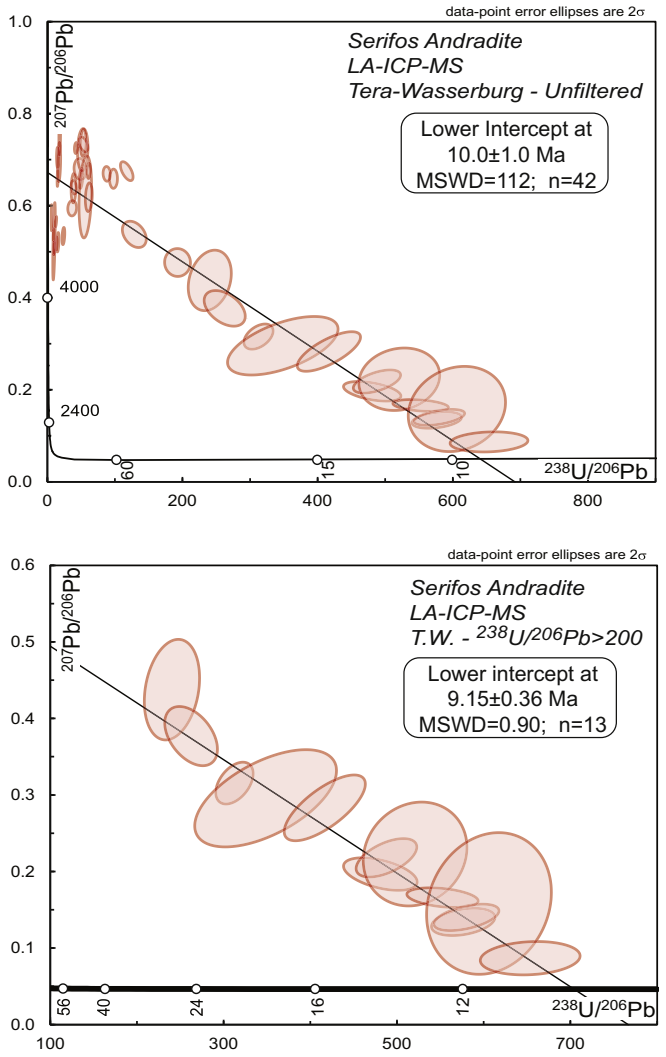

Fig. 8. U-Pb results for Serifos Andradite plotted on Tera-Wasserburg concordia. A) All U/Pb ratios plotted and regressed from analyzed fragments. The large uncertainty results from scattered low U/Pb analyses. B) A more precise lower intercept with 4% 2σ uncertainty and MSWD < 1 results when only $^{238}U/^{206}Pb$ > 200 analyses are utilized in the regression. This date falls directly between the youngest zircon U-Pb ages from the Serifos Granodiorite and Rb-Sr biotite dates.

related pluton remains the simplest the approach. In settings with prolonged intrusive histories, such as continental arcs, establishing this genetic link can be problematic. Examples of prolonged intrusive and hydrothermal histories are known from the Variscan belt of Spain as well as the Sierra Nevada arc of western North America (Tornos et al., 2000; D'Errico et al., 2012). Age data from both grandite and pluton can form this genetic link. Mali grandite offers a simple example of the utility of grandite U-Pb geochronology. The sample is sourced from alluvial deposits disconnected from potential causative plutons, but U-Pb age data link it to CAMP age intrusions throughout the region.

The timing of hydrothermal activity is a key factor in any predictive genetic model of skarn systems. The short lifespans of pluton-related hydrothermal systems, perhaps tens of thousands to at most a few millions of years, makes a definitive chronology difficult to produce (Chiaradia et al., 2013; Chelle-Michou et al., 2015). Zircon U-Pb geochronology can produce a high-resolution record of the pluton emplacement history. $^{40}Ar/^{39}Ar$ dating of micas, etc. are difficult to link to a specific phase of hydrothermal activity and may be thermally reset by subsequent pulses of magmatism (Chiaradia et al., 2013). Titanite U-Pb geochronology has been employed as well to date mineralization, as its high closure temperature (~600–700 °C) prevents subsequent resetting (Li et al., 2010), but titanite is not nearly as ubiquitous as grandite in this setting. Re-Os molybdenite geochronometry has been applied extensively to date mineralization (see Stein et al., 2001), but, similar to titanite, does not occur as widely as grandite.

Precision of the method must be taken into account when discussing the applicability of any geochronometric system. The single-percent uncertainties associated with grandite U-Pb limits its resolving power when an episode of skarn formation and hydrothermal activity may only span tens of thousands to a few million year. As shown in the Serifos Island case study, Neogene skarn systems are desirable for this method as percent level uncertainties may approach as low as a few tens of thousands of years at this age range. Preferentially selecting grandites for high [U] will also increase the precision of U-Pb dates. The exact mechanism of U incorporation into grandite remains unclear despite numerous studies (Yudintsev et al., 2002; Rák et al., 2011; Guo et al., 2016). Of the garnets surveyed in this study, higher andradite content correlates with [U], with the exception of Mali Red Grandite. This agrees with the study of Rák et al., 2011 which argues for a coupled substitution mechanism allowing for the incorporation of U into andradite. However, Smith et al., 2004 shows U enrichment does not correlate strictly with andradite content, but rather, [REE]. U mobility in hydrothermal fluids is a function of fO2. Smith et al., 2004 suggests that U and REE incorporation into garnet is controlled by a reduction in fO2, and a corresponding reduction in solubility, as magmatically-buffered hydrothermal fluids interact with skarn assemblages. This leads to disequilibrium partitioning of U and REE into garnet governed primarily by surfaces sorption processes. However, this study notes that the highest observed [U] are consistently found within andradite-rich rims of grandites.

Another approach to increase precision is to employ microdrillling coupled with ID-TIMS methods. Microsampling of garnets for Sm-Nd geochronology has been applied very successfully (Pollington and Baxter, 2011; Dragovic et al., 2012), but the U-Pb system has several advantages over Sm-Nd. Whole rock or matrix analysis to produce an isochron is not necessary for a U-Pb age determination. Partial dissolution is also not required to remove inclusions, as Pbc from inclusions can be corrected for directly by measuring ^{204}Pb. Zircon, the most problematic possible U-rich inclusion as it may record older dates than grandite, will not be dissolved using a standard table-top dissolution methods. Fraction size is the only limiting factor as low [U], Neogene grandite may require tens of milligrams of material to yield reasonable precision. As skarn-derived garnets are often centimeters in diameter, such fraction sizes are not prohibitive. Previous efforts in garnet microsampling have focused on determining garnet growth rates in regional metamorphic environments (Christensen et al., 1989; Vance and O'nions, 1990; Pollington and Baxter, 2011; Dragovic et al., 2012). Grandite U-Pb could potentially bring the same absolute timing constraints to these more ephemeral systems.

7. Conclusions

Grossular-andradite garnet yields U-Pb age data of similar precision and quality to apatite and titanite. Current precision levels for LA-ICPMS data are on the 1–10% level, while uncertainties for TIMS data for Mesozoic and Proterozoic grandites are ~1%. All grandites discussed here produce dates consistent with other chronometers and regional geology. This study proposes Willsboro Andradite as a potential reference standard for the method, but it requires more extensive ID-TIMS U-Pb dating to produce robust reference ages. Unfiltered LA-ICPMS U-Pb age data from Serifos Island skarn andradite yields data in agreement with other U-Pb, $^{40}Ar/^{39}Ar$, Rb-Sr, and (U-Th)/He chronometers from the island. When this data is further filtered based on $^{238}U/^{206}Pb$ ratio, it yields an age of 9.15 ± 0.36 Ma (MSWD = 0.9; n = 13), which falls directly in between the youngest zircon U-Pb dates and biotite Rb-Sr dates from the Serifos Granodiorite. When combined with other methods, U-Pb geochronology of grossular-

andradite garnet has the potential to refine the understanding of the temporal evolution of magmatic hydrothermal systems.

Supplementary data to this article can be found online at http://dx.doi.org/10.1016/j.chemgeo.2017.04.020.

Acknowledgements

We would like to thank Michelle Gevedon and Stephanie Wafforn for their support in developing the method and for many fruitful discussions. We would also like to thank Jade Star Lackey for providing samples of Willsboro Andradite. Doug Walker, Jason Hallman, and Joe Andrew provided welcome assistance with ID-TIMS analysis at the University of Kansas. Formal reviews by K. Mezger, D. Chew, and an anonymous reviewer greatly improved this work. This manuscript also benefited from informal reviews by J. Barnes, A. Smye, E. Baxter and M. Cloos. LA-ICPMS U-Pb data can be found in Supplementary Table 1. LA-ICPMS trace element data can be found in Supplementary Table 2.

References

Altherr, R., Kreuzer, H., Wendt, I., Lenz, H.N., Wagner, G., Keller, J., Harre, W., Hohndorf, A., 1982. A late Oligocene/early Miocene high temperature belt in the Attic-Cycladic crystalline complex (SE Pelagonian, Greece). Geologisches Jahrbuch E 23, 97–164.

Barker, D.S., 1977. Northern trans-Pecos magmatic province: introduction and comparison with the Kenya rift. Geol. Soc. Am. Bull. 88, 1421–1427.

Basu, A., Faggert, B., Sharma, M., 1988. Sm–Nd isotopic study of wollastonite skarn and garnet amphibolite metamorphism in the Adirondack Mountains, New York. Eos 69, 468.

Blackburn, T.J., 2006. Development of new applications in volcanic (U-Th)/He geochronology. (Doctoral dissertation, University of Kansas).

Blackburn, T.J., Stockli, D.F., Walker, J.D., 2007. Magnetite (U–Th)/He dating and its application to the geochronology of intermediate to mafic volcanic rocks. Earth Planet. Sci. Lett. 259, 360–371.

Bloomfield, K., Cépeda-Dávila, L., 1973. Oligocene alkaline igneous activity in NE Mexico. Geol. Mag. 110, 551–555.

Bowring, S.A., Erwin, D., Parrish, R., Renne, P., 2005. EARTHTIME: a community-based effort towards high-precision calibration of earth history. Geochim. Cosmochim. Acta 69, A316.

Bowring, J., McLean, N.M., Bowring, S., 2011. Engineering cyber infrastructure for U-Pb geochronology: Tripoli and U-Pb_Redux. Geochem. Geophys. Geosyst. 12.

Caddick, M.J., Konopásek, J., Thompson, A.B., 2010. Preservation of garnet growth zoning and the duration of prograde metamorphism. J. Petrol. 51, 2327–2347.

Chelle-Michou, C., Chiaradia, M., Selby, D., Ovtcharova, M., Spikings, R.A., 2015. High-resolution geochronology of the Coroccohuayco porphyry-skarn deposit, Peru: a rapid product of the Incaic orogeny. Econ. Geol. 110, 423–443.

Chew, D., Petrus, J., Kamber, B., 2014. U–Pb LA–ICPMS dating using accessory mineral standards with variable common Pb. Chem. Geol. 363, 185–199.

Chiaradia, M., Schaltegger, U., Spikings, R., Wotzlaw, J.-F., Ovtcharova, M., 2013. How accurately can we date the duration of magmatic-hydrothermal events in porphyry systems?—an invited paper. Econ. Geol. 108, 565–584.

Christensen, J.N., Rosenfeld, J.L., DePaolo, D.J., 1989. Rates of tectonometamorphic processes from rubidium and strontium isotopes in garnet. Science 244, 1465.

Clark, K.F., Foster, C.T., Damon, P.E., 1982. Cenozoic mineral deposits and subduction-related magmatic arcs in Mexico. Geol. Soc. Am. Bull. 93, 533–544.

Clechenko, C., Valley, J., 2003. Oscillatory zoning in garnet from the Willsboro Wollastonite Skarn, Adirondack Mts, New York: a record of shallow hydrothermal processes preserved in a granulite facies terrane. J. Metamorph. Geol. 21, 771–784.

Clechenko, C.C., Valley, J.W., Hamilton, M.A., McLelland, J.M., Bickford, M., 2002. Shrimp II geochronology of the Adirondack AMCG suite: timing and depth of emplacement of anorthosite in the northeastern Adirondacks. In: 2002 Denver Annual Meeting.

Condon, D., Schoene, B., McLean, N., Bowring, S., Parrish, R., 2015. Metrology and traceability of U–Pb isotope dilution geochronology (EARTHTIME Tracer Calibration Part I). Geochim. Cosmochim. Acta 164, 464–480.

Crowe, D.E., Riciputi, L.R., Bezenek, S., Ignatiev, A., 2001. Oxygen isotope and trace element zoning in hydrothermal garnets: windows into large-scale fluid-flow behavior. Geology 29, 479–482.

Deckart, K., Clark, A.H., Celso, A.A., Ricardo, V.R., Bertens, A.N., Mortensen, J.K., Fanning, M., 2005. Magmatic and hydrothermal chronology of the giant Rio Blanco porphyry copper deposit, central Chile: implications of an integrated U-Pb and 40Ar/39Ar database. Econ. Geol. 100, 905–934.

D'Errico, M.E., Lackey, J.S., Surpless, B.E., Loewy, S.L., Wooden, J.L., Barnes, J.D., Strickland, A., Valley, J.W., 2012. A detailed record of shallow hydrothermal fluid flow in the Sierra Nevada magmatic arc from low-δ18O skarn garnets. Geology 40, 763–766.

DeWolf, C., Zeissler, C.J., Halliday, A., Mezger, K., Essene, E., 1996. The role of inclusions in U-Pb and Sm-Nd garnet geochronology: stepwise dissolution experiments and trace uranium mapping by fission track analysis. Geochim. Cosmochim. Acta 60, 121–134.

Dragovic, B., Samanta, L.M., Baxter, E.F., Selverstone, J., 2012. Using garnet to constrain the duration and rate of water-releasing metamorphic reactions during subduction: an example from Sifnos, Greece. Chem. Geol. 314–317, 9–22.

Duchêne, S., Blichert-Toft, J., Luais, B., Télouk, P., Lardeaux, J., Albarede, F., 1997. The Lu-Hf dating of garnets and the ages of the Alpine high-pressure metamorphism. Nature 387, 586–588.

Ducoux, M., Branquet, Y., Jolivet, L., Arbaret, L., Grasemann, B., Rabillard, A., Gumiaux, C., Drufin, S., 2017. Synkinematic skarns and fluid drainage along detachments: the West Cycladic Detachment System on Serifos Island (Cyclades, Greece) and its related mineralization. Tectonophysics 695, 1–26.

Dürr, S., Altherr, R., Keller, J., Okrusch, M., Seidel, E., 1978. The median Aegean crystalline belt: stratigraphy, structure, metamorphism, magmatism. In: Alps, Apennines, Hellenides. 38. pp. 455–476.

Furon, R., Hallam, A., Stevens, L.A., 1963. Geology of Africa. Oliver & Boyd London.

Grasemann, B., Schneider, D.A., Stockli, D.F., Iglseder, C., 2011. Miocene bivergent crustal extension in the Aegean: evidence from the western Cyclades (Greece). Lithosphere 4, 23–39.

Guo, X., Navrotsky, A., Kukkadapu, R.K., Engelhard, M.H., Lanzirotti, A., Newville, M., Ilton, E.S., Sutton, S.R., Xu, H., 2016. Structure and thermodynamics of uranium-containing iron garnets. Geochim. Cosmochim. Acta 189, 269–281.

Haack, U.K., Gramse, M., 1972. Survey of garnets for fossil fission tracks. Contrib. Mineral. Petrol. 34, 258–260.

Hamilton, M.A., McLelland, J., Selleck, B., 2004. SHRIMP U-Pb zircon geochronology of the anorthosite-mangerite-charnockite-granite suite, Adirondack Mountains, New York: ages of emplacement and metamorphism. Geol. Soc. Am. Mem. 197, 337–355.

Hart, N.R., Stockli, D.F., Hayman, N.W., 2016. Provenance evolution during progressive rifting and hyperextension using bedrock and detrital zircon U-Pb geochronology, Mauléon Basin, western Pyrenees. Geosphere 12 (4), 1166–1186.

Harvey, J., Baxter, E.F., 2009. An improved method for TIMS high precision neodymium isotope analysis of very small aliquots (1–10 ng). Chem. Geol. 258, 251–257.

Henry, C.D., Price, J.G., 1984. Variations in caldera development in the Tertiary volcanic field of trans-Pecos Texas. J. Geophys. Res. Solid Earth 89, 8765–8786.

Horstwood, M.S., Košler, J., Gehrels, G., Jackson, S.E., McLean, N.M., Paton, C., Pearson, N.J., Sircombe, K., Sylvester, P., Vermeesch, P., 2016. Community-derived standards for LA-ICP-MS U-(Th-) Pb geochronology–uncertainty propagation, age interpretation and data reporting. Geostand. Geoanal. Res. 40, 311–332.

Iglseder, C., Grasemann, B., Schneider, D.A., Petrakakis, K., Miller, C., Klötzli, U.S., Thöni, M., Zámolyi, A., Rambousek, C., 2009. I and S-type plutonism on Serifos (W-Cyclades, Greece). Tectonophysics 473, 69–83.

Jamtveit, B., Wogelius, R.A., Fraser, D.G., 1993. Zonation patterns of skarn garnets: records of hydrothermal system evolution. Geology 21, 113–116.

Johnson, M., Boehm, E., Krupp, H., Zang, J., Kammerling, R., 1995. Gem-quality grossular-andradite: a new garnet from Mali. Gems Gemol. 31, 152–166.

Krogh, T., 1973. A low-contamination method for hydrothermal decomposition of zircon and extraction of U and Pb for isotopic age determinations. Geochim. Cosmochim. Acta 37, 485–494.

Lal, N., Nagpaul, K., Sharma, K., 1976. Fission-track ages and uranium concentration in garnets from Rajasthan, India. Geol. Soc. Am. Bull. 87, 687–690.

Lee, C.-T.A., Lackey, J.S., 2015. Global continental arc flare-ups and their relation to long-term greenhouse conditions. Elements 11, 125–130.

Lee, C.-T.A., Shen, B., Slotnick, B.S., Liao, K., Dickens, G.R., Yokoyama, Y., Lenardic, A., Dasgupta, R., Jellinek, M., Lackey, J.S., 2013. Continental arc–island arc fluctuations, growth of crustal carbonates, and long-term climate change. Geosphere 9, 21–36.

Li, J.-W., Deng, X.-D., Zhou, M.-F., Liu, Y.-S., Zhao, X.-F., Guo, J.-L., 2010. Laser ablation ICP-MS titanite U–Th–Pb dating of hydrothermal ore deposits: a case study of the Tonglushan Cu–Fe–Au skarn deposit, SE Hubei Province, China. Chem. Geol. 270, 56–67.

Maksaev, V., Munizaga, F., McWilliams, M., Fanning, M., Mathur, R., Ruiz, J., Zentilli, M., 2004. New chronology for El Teniente, Chilean Andes, from U/Pb, 40Ar/39Ar, Re/Os and fission-track dating: implications for the evolution of a supergiant porphyry Cu-Mo deposit. In: Andean Metallogeny: New Discoveries, Concepts Update. 11. Society of Economic Geologists, pp. 15–54 (Special Publication).

Marinos, G., 1951. Geology and metallogeny of Serifos island. In: IGME Geological and Geophysical Research Athens I, pp. 95–127.

Marsh, J.H., Stockli, D.F., 2015. Zircon U–Pb and trace element zoning characteristics in an anatectic granulite domain: Insights from LASS-ICP-MS depth profiling. Lithos 239, 170–185.

Marzoli, A., Renne, P.R., Piccirillo, E.M., Ernesto, M., Bellieni, G., De Min, A., 1999. Extensive 200-million-year-old continental flood basalts of the Central Atlantic Magmatic Province. Science 284, 616–618.

McLean, N.M., Bowring, J.F., Bowring, S.A., 2011. An algorithm for U-Pb isotope dilution data reduction and uncertainty propagation. Geochm. Geophys. Geosyst. 12 (6).

McLean, N.M., Condon, D.J., Schoene, B., Bowring, S.A., 2015. Evaluating uncertainties in the calibration of isotopic reference materials and multi-element isotopic tracers (EARTHTIME Tracer Calibration Part II). Geochim. Cosmochim. Acta 164, 481–501.

McLelland, J., Daly, J.S., McLelland, J.M., 1996. The Grenville orogenic cycle (ca. 1350–1000 Ma): an Adirondack perspective. Tectonophysics 265, 1–28.

McLelland, J., Hamilton, M., Selleck, B., McLelland, J., Walker, D., Orrell, S., 2001. Zircon U-Pb geochronology of the Ottawan orogeny, Adirondack highlands, New York: regional and tectonic implications. Precambrian Res. 109, 39–72.

Meinert, L.D., 1992. Skarns and skarn deposits. Geosci. Can. 19.

Meinert, L.D., Nicolessus, S., Mortenses, J., Cornell, D.H., 2001. U-Pb dating of hydrothermal garnets from skarn deposits: implication for petrogenesis and ore deposits. In: General Meeting.

Mezger, K., Hanson, G., Bohlen, S., 1989. U-Pb systematics of garnet: dating the growth of garnet in the Late Archean Pikwitonei granulite domain at Cauchon and Natawahunan Lakes, Manitoba, Canada. Contrib. Mineral. Petrol. 101, 136–148.

Mezger, K., Rawnsley, C., Bohlen, S., Hanson, G., 1991. U-Pb garnet, sphene, monazite,

and rutile ages: implications for the duration of high-grade metamorphism and cooling histories, Adirondack Mts., New York. J. Geol. 415–428.
Norman, M., Pearson, N., Sharma, A., Griffin, W., 1996. Quantitative analysis of trace elements in geological materials by laser ablation ICPMS: instrumental operating conditions and calibration values of NIST glasses. Geostand. Newslett. 20, 247–261.
Paton, C., Hellstrom, J., Paul, B., Woodhead, J., Hergt, J., 2011. Iolite: freeware for the visualisation and processing of mass spectrometric data. J. Anal. At. Spectrom. 26, 2508–2518.
Petrus, J.A., Kamber, B.S., 2012. VizualAge: a novel approach to laser ablation ICP-MS U-Pb geochronology data reduction. Geostand. Geoanal. Res. 36, 247–270.
Pollington, A.D., Baxter, E.F., 2011. High precision microsampling and preparation of zoned garnet porphyroblasts for Sm–Nd geochronology. Chem. Geol. 281, 270–282.
Rák, Z., Ewing, R.C., Becker, U., 2011. Role of iron in the incorporation of uranium in ferric garnet matrices. Phys. Rev. B 84, 155128.
Reiners, P.W., 2005. Zircon (U-Th)/He thermochronometry. Rev. Mineral. Geochem. 58, 151–179.
Rocha, H., De Leon, J., Romero, S., 1986. I'Vesuvianita y grossular de Lago Jaco. Boletin de Mineralogia 2, 41–59.
Salemink, J., 1985. Skarn and ore formation at Seriphos, Greece as a consequence of granodiorite intrusion. Geol. Ultraiect. 40, 1–232.
Salemink, J., Schuiling, R., 1987. A two-stage, transient heat and mass transfer model for the granodiorite intrusion at Seriphos, Greece, and the associated formation of contact metasomatic skarn and Fe-ore deposits. In: Chemical Transport in Metasomatic Processes. Springer, pp. 547–575.
Schmitz, M.D., Bowring, S.A., 2001. U-Pb zircon and titanite systematics of the Fish Canyon Tuff: an assessment of high-precision U-Pb geochronology and its application to young volcanic rocks. Geochim. Cosmochim. Acta 65, 2571–2587.
Sebai, A., Feraud, G., Bertrand, H., Hanes, J., 1991. 40 Ar/39 Ar dating and geochemistry of tholeiitic magmatism related to the early opening of the Central Atlantic rift. Earth Planet. Sci. Lett. 104, 455–472.
Seman, S., Stockli, D.F., Smye, A.J., Hernandez-Goldstein, E., 2014. In: Garnet (U-Th)/He thermochronometry and its application to exhumed high-pressure low-temperature metamorphic rocks, Thermo2014. 14th International Conference on Thermochronology, Chamonix, France.
Smith, M., Henderson, P., Jeffries, T., Long, J., Williams, C., 2004. The rare earth elements and uranium in garnets from the Beinn an Dubhaich Aureole, Skye, Scotland, UK: constraints on processes in a dynamic hydrothermal system. J. Petrol. 45, 457–484.
Smye, A.J., Stockli, D.F., 2014. Rutile U–Pb age depth profiling: a continuous record of lithospheric thermal evolution. Earth Planet. Sci. Lett. 408, 171–182.
Stein, H., Markey, R., Morgan, J., Hannah, J., Scherstén, A., 2001. The remarkable Re–Os chronometer in molybdenite: how and why it works. Terra Nova 13, 479–486.
Tagami, T., Farley, K.A., Stockli, D.F., 2003. (U–Th)/He geochronology of single zircon grains of known Tertiary eruption age. Earth Planet. Sci. Lett. 207, 57–67.
Tornos, F., Delgado, A., Casquet, C., Galindo, C., 2000. 300 million years of episodic hydrothermal activity: stable isotope evidence from hydrothermal rocks of the Eastern Iberian Central System. Mineral. Deposita 35, 551–569.
Valley, J.W., 1985. olymetamorphism in the Adirondacks: wollastonite at contacts of shallowly intruded anorthosite. In: The Deep Proterozoic Crust in the North Atlantic Provinces. Springer, pp. 217–236.
Valley, J.W., Bohlen, S.R., Essene, E.J., Lamb, W., 1990. Metamorphism in the Adirondacks: II. The role of fluids. J. Petrol. 31, 555–596.
Vance, D., O'nions, R., 1990. Isotopic chronometry of zoned garnets: growth kinetics and metamorphic histories. Earth Planet. Sci. Lett. 97, 227–240.
Verati, C., Bertrand, H., Féraud, G., 2005. The farthest record of the Central Atlantic Magmatic Province into West Africa craton: precise 40 Ar/39 Ar dating and geochemistry of Taoudenni basin intrusives (northern Mali). Earth Planet. Sci. Lett. 235, 391–407.
Vermeesch, P., 2010. HelioPlot, and the treatment of overdispersed (U–Th–Sm)/He data. Chem. Geol. 271, 108–111.
Yao, Y., Chen, J., Lu, J., Wang, R., Zhang, R., 2014. Geology and genesis of the Hehuaping magnesian skarn-type cassiterite-sulfide deposit, Hunan Province, Southern China. Ore Geol. Rev. 58, 163–184.
Yudintsev, S.V., Lapina, M.I., Ptashkin, A.G., Ioudintseva, T.S., Utsunomiya, S., Wang, L.M., Ewing, R.C., 2002. Accommodation of Uranium Into the Garnet structure, MRS Proceedings. 28. Cambridge Univ Presspp. JJ11.
Zhai, D.-G., Liu, J.-J., Zhang, H.-Y., Wang, J.-P., Su, L., Yang, X.-A., Wu, S.-H., 2014. Origin of oscillatory zoned garnets from the Xieertala Fe–Zn skarn deposit, northern China: in situ LA–ICP-MS evidence. Lithos 190, 279–291.